Spin Experiments—Technological Challenges and Selected Physics Highlights

K. Rith

Citation: AIP Conference Proceedings **1149**, 21 (2009); doi: 10.1063/1.3215632
View online: https://doi.org/10.1063/1.3215632
View Table of Contents: http://aip.scitation.org/toc/apc/1149/1
Published by the American Institute of Physics

Spin Experiments - Technological Challenges and Selected Physics Highlights

K. Rith

DESY, Notkestrasse 85, 22603 Hamburg, Germany and University of Erlangen-Nürnberg, Physikalisches Institut, Erwin-Rommel-Str. 1, 91058 Erlangen, Germany

Abstract. Selected highlights in experimental spin physics are presented and dicussed.

INTRODUCTION

During the last two decades spin physics has made enormous progress. New high-precision experiments required substantially increased luminosities and beam and target polarizations. They profited very much from the many achievements in the technologies of polarized sources, beams and targets, which have been discussed in many contributions to this conference. In this contribution I will address shortly those achievements and then discuss a selection of highlights in experimental spin physics reflecting my personal taste. Due to lack of space I can only mention and cite a small fraction the experimental results and refer the reader to the corresponding contributions to this conference.

TECHNOLOGICAL ACHIEVEMENTS

Examples for the many technological achievements, which were the prerequisites for todays high-precision experiments are:

- strained-surface photocathode GaAs polarized electron sources, which nowadays routinely provide high current electron beams with polarizations $p_e \geq 0.8$, recently even around 0.9;
- high beam polarization in high-energy electron/positron storage rings. The degree of polarization depends critically on the machine energy and magnet alignment. At LEP the precise measurement of the beam energy by resonant depolarization of the transversely polarized beam [1] was crucial to reduce the uncertainty in the measurement of the Z^0 mass to its present low value of only 2.1 MeV. At HERA longitudinal polarization was provided for HERMES, H1 and ZEUS by systems of spin-rotators upstream and downstream of the experiments. Until the year 2000 polarization values of about 0.6 [2, 3] were routinely achieved;
- high flux polarized ion sources [4];

CP1149, *Spin Physics, 18th International Spin Physics Symposium*
edited by D. G. Crabb, D. B. Day, S. Liuti, X. Zheng, M. Poelker, and Y. Prok

- internal storage-cell polarized $\vec{H}$, $\vec{D}$, and $^3\vec{He}$ atomic gas targets [5] with a large fraction f of polarizable nucleons and a high degree of polarization ($f \cong 1$ and $p_T \geq 0.8$ for H and D);
- large polarized kryogenic targets [6];
- polarized proton beams in storage rings like the IUCF cooler ring, COSY or RHIC. The RHIC accelerator complex [7] contains a system of several full and partial Siberian Snakes both in the AGS and in RHIC to overcome depolarizing resonances and to preserve polarization during ramping of the beam energy. Average polarizations of about 0.6 have been achieved so far at a beam energy of 100 GeV for a running period of more than a month. In my view RHIC is a masterpiece of accelerator physics;
- fast and precise polarimeters.

Challenging projects for the next generation of accelerators and experiments are the development of

- high current polarized positron sources for the Next Linear Collider [8],
- polarized anti-proton beams for the anti-proton facility FAIR at GSI [9].

SELECTED PHYSICS HIGHLIGHTS

Highlight 1: A_{LR}^f from SLD A new era of experiments with polarized electron beams started with the development of electron sources with strained GaAs photo-cathode surfaces for the SLC which allowed to overcome the GaAs polarization limit of $p_{e,max} = 0.5$. After optimization of source laser wavelength a beam polarization of $p_e \cong 0.65$ was achieved in 1993 which was increased to $p_e \cong 0.80$ from 1994 onwards [10].

Only the electron beam was polarized. This allowed the measurement of the left-right asymmetry A_{LR}^fin the reaction $\vec{e^-}_{L,R}e^+ \longrightarrow f\bar{f}$, which is related to the weak vector and axial coupling of fermions of type f to the Z^0, $g_{V,f}$ and $g_{A,f}$.

Since longitudinal electron polarization was only available at SLC and not at LEP all the information on such left-right asymmetries listed in the Review of Particle Physics [11] is based on measurements at SLD. For $f \equiv e^-$ one obtains $g_{V,e-}/g_{A,e-} = 1 - 4sin^2\theta_W$, where θ_W is the Weinberg angle. These SLD measurements resulted in the statistically most precise single determination of $sin^2\theta_W$:

$$sin^2\theta_W(M_Z) = 0.23098 \pm 0.00026. \quad (1)$$

Highlight 2: PV in Moeller scattering Such polarized electron sources became standard equipment at essentially all electron facilities like AMPS and Bates (which meanwhile both were shut down), ELSA, JLAB, MAMI, JPARC, and others. Sophisticated photo-cathode surface structures (e.g. gradient-doped strained superlattice) were developed to overcome the charge limit and to achieve high polarization.

First measurements of parity violation (PV) in $\vec{e^-}_{L,R}e^- \longrightarrow e^-e^-$ were performed by E158 [12], the last fixed-target experiment at SLAC. A very high beam polarization of

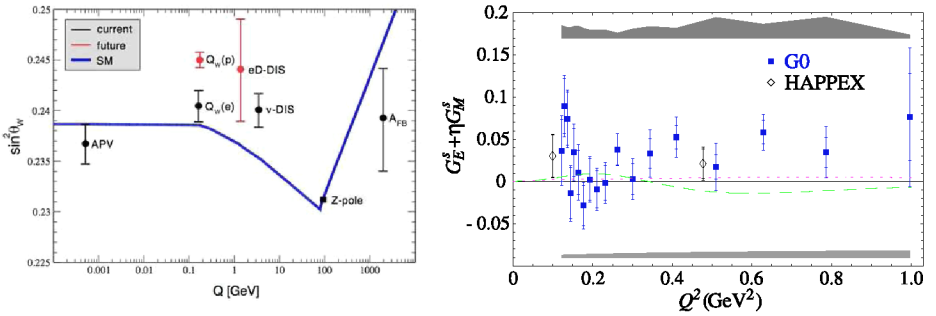

FIGURE 1. Left panel: $sin^2\theta_W$ as a function of momentum transfer Q (this figure is taken from the Review of Particle Physics [11]; Right panel: World data for $G_E^s + \eta G_M^s$ as a function of Q^2.

$p_e = 0.89 \pm 0.04$ was achieved. All beam-helicity related systematics had to be very precisely controlled, since the PV amplitude due to the electroweak interference of one-photon and Z^0 exchange was measured to be only

$$A_{PV} = A(Q^2,y)[1 - sin^2\theta_W^{eff}(Q)] = [-1.31 \pm 0.14(stat) \pm 0.10(sys)]10^{-7}, \quad (2)$$

corresponding to

$$sin^2\theta_W^{eff}(Q) = 0.2397 \pm 0.0010 \pm 0.0008. \quad (3)$$

The result is shown in the left panel of Fig. 1. It is 6.2σ away from the value at the Z^0 pole and demonstrates the running of the Weinberg-angle in perfect agreement with SM predictions.

Highlight 3: Parity violation in electron-nucleon scattering - Nucleon Strange Form Factors Parity violation in elastic electron-nucleon scattering has been measured with very high precision by several experiments (SAMPLE/BATES, G0/JLAB, HAPPEX/JLAB, A4/MAMI) with the aim to determine the contribution of strange quarks, G_E^s and G_M^s, to the electric and magnetic form factors of the nucleon. Very small asymmetries of O(10^6) have been obtained, from which the quantity $G_E^s + \eta G_M^s$, has been extracted, where η is a kinematical factor. Recent results for this quantity [13] are shown in the right panel of Fig.1 as a function of Q^2. For a recent discussion of the extraction of G_E^s and G_M^s see for example Refs. [14, 15].

Highlight 4: Total polarized CC electron-nucleon scattering cross section The two collider experiments H1 [16] and ZEUS [17] at HERA measured the polarization dependence of the cross-section for the charged-current (CC) interaction $\vec{e}_{L,R}p \longrightarrow \nu X$ for both incident electrons and positrons. The standard model (SM) predicts that the CC cross-section for right-handed electrons and for left-handed positrons vanishes and that the polarization dependence of the cross section is given by:

$$\sigma_{e^\pm p}^{CC} = (1 \pm P_e)\sigma_{e^\pm p}^{CC}(P_e = 0), \quad (4)$$

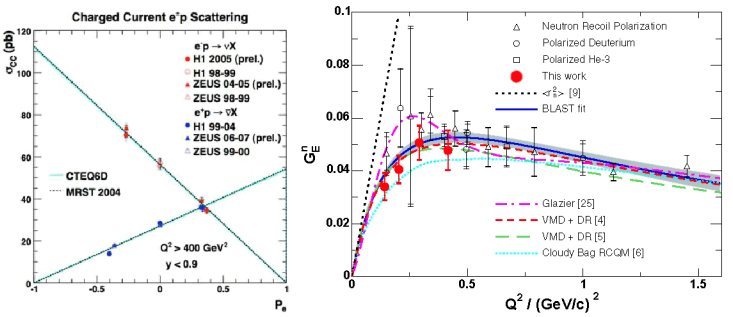

FIGURE 2. Left panel: ZEUS and H1 results for the deep-inelastic CC cross section for e^- and e^+ as a function of longitudinal beam polarization; Right panel: World data for G_E^n from double-polarization experiments as a function of Q^2 .

where the positive (negative) sign in the first bracket on the right-hand side of the equation holds for positrons (electrons) and $P_e = N_R - N_L / N_R + N_L$. The results of these measurements are shown in the left panel of Fig. 2 as a function of P_e.

This textbook plot demonstrates nicely the agreement with the SM. There is no sign of right-handed charged currents. Furthermore the data can be used to set a limit on the mass of a right-handed W: $m_{W,R} > 208\ GeV$ [16].

Highlight 5: Precise determination of G_E^n from double-spin experiments As already discussed in detail by E. Leader [18] recent measurements of the Q^2 dependence of the electric proton form factor, $G_E^p(Q^2)$, showed surprising differences between the Rosenbluth method, used for nearly half a century for the extraction of G_E^p and G_M^p, and the method based on the measurement of the polarization of the recoiling proton [19]. These differences might be related to contributions of two-photon exchange in the elastic scattering process [20]. The measurement of the small electric form factor of the neutron, G_E^n is rather difficult. Early measurements using the Rosenbluth method even resulted in negative values of $(G_E^n)^2$ [21].

Double-polarization experiments, where longitudinally polarized electrons are either scattered off a longitudinally polarized Deuterium or ^3He target or off an unpolarized liquid deuterium target and the polarization of the recoiling neutron is measured, offer a clean possibility to determine G_E^n as in this case it enters linearly in the asymmetry.

Recent results [22] of the Q^2 dependence of G_E^n, obtained by the double-polarization technique are shown in the right panel of Fig. 2.

Highlight 6: Asymmetries in polarized pp scattering at low energies The power of polarization experiments with internal polarized gas targets in storage rings is demonstrated by the measurements of the angular distributions of various spin-correlation parameters in elastic $\vec{p}\vec{p}$ scattering by the PINTEX collaboration at the Indiana cooler ring[23]. Data were taken for eight beam energies between 197 MeV and 445. Previously these distributions were essentially terra incognita while now the data points cover the angular range up to 45 degrees like a chain of pearls.

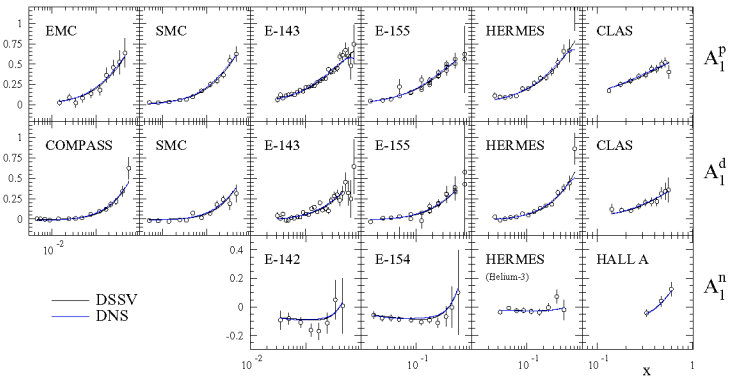

FIGURE 3. World data for the double-spin virtual-photon asymmetry $A_1(x)$ for proton, deuteron and neutron measured in polarized deep-inelastic charged-lepton nucleon scattering.

Highlight 7: Asymmetries in polarized DIS Most of the present experimental information about the spin structure of the nucleon is based on the measurement of double-spin asymmetries (DSA) in deep-inelastic scattering (DIS), of longitudinally polarized charged leptons from longitudinally polarized targets, $\vec{l}\vec{N} \longrightarrow l'X$. A detailed discussion of the underlying physics, the various experiments, the experimental results, and their theoretical interpretation can be found in the recent review by Burkardt, Miller and Nowak [24].

The experimental information from inclusive polarized DIS experiments is summarized in Fig. 3, where the virtual-photon asymmetry $A_1(x)$ for proton, deuteron and neutron is shown as a function of the Bjorken variable x [25]. From these asymmetries one obtains the spin-dependent structure function $g_1(x) = 1/2 \sum_q e_q^2 q(x)$, where the sum runs over all quark and anti-quark flavors, e_q is the charge of the quark (anti-quark) in units of the elementary charge $\mid e \mid$ and $q(x)$ is the quark (anti-quark) helicity distribution function (DF) (for simplicity the additional dependence on the squared four-momentum transfer Q^2 is omitted here), and also the quantity $\Delta\Sigma$, which in the $\bar{MS}$-scheme can be interpreted as the fractional contribution of quark spins to the spin of the nucleon.

From their high statistics data taken with a polarized deuteron target, both HERMES and COMPASS have recently determined $\Delta\Sigma$ in NLO-QCD and the $\bar{MS}$-scheme. The HERMES result [26] $\Delta\Sigma = 0.330 \pm 0.025(stat) \pm \pm 0.030(sys)$ was obtained from the fractional first moment of $g_1^d(x)$ under the assumption that g_1^d vanishes for x-values below the x-range covered by the data. The COMPASS result [27] $\Delta\Sigma = 0.30 \pm 0.010(stat) \pm 0.020(syst)$ was obtained from a NLO-QCD fit to the data. The two results agree nicely within their uncertainties They have much higher precision than the original EMC result [28] $\Delta\Sigma = 0.12 \pm 0.09 \pm 0.14$ and we can safely conclude that quark spins contribute only about one third to the spin of the nucleon.

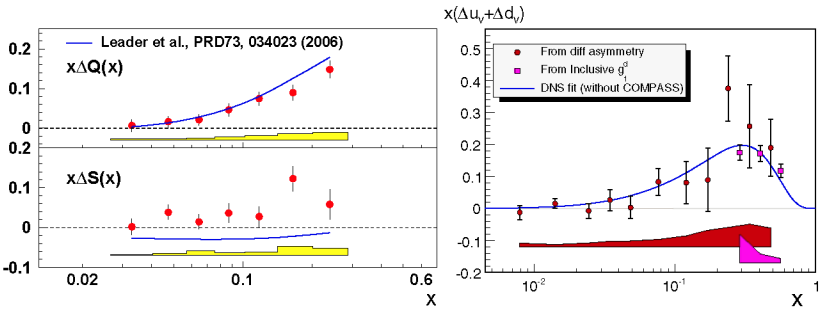

FIGURE 4. Left panel: HERMES results for the strange-quark helicity distribution; Right panel: COMPASS results for the helicity distribution of valence quarks.

Highlight 8: Quark helicity distributions Information about the flavor-separated quark (anti-quark) helicity DFs can be obtained from DSAs in semi-inclusive polarized DIS experiments, $\vec{l}N \longrightarrow l'hX$ where in addition to the scattered lepton also (identified) hadrons h are detected. Such data have been published some time ago by HERMES [29]. $\Delta u(x)$ is positive, $\Delta d(x)$ is negative and the sea-quark helicity DFs are compatible with zero within their uncertainties. New results, which shed more light on the sea-quark DFs have been recently published by HERMES and COMPASS. They are presented in Fig. 4. The left panel shows the HERMES result [30] for the strange-quark helicity DF, $x\Delta s(x)$, obtained from the semi-inclusive asymmetry of the *sum* of positive and negative kaons. The first partial moment in the measured x-range [0.02,0.6] $\Delta s = 0.037 \pm 0.019 \pm 0.027$ is rather different from the result derived from the inclusive deuteron data within SU(3): $\Delta s = -0.85 \pm 0.019 \pm 0.027$. Probably this is due to a negative contribution from the unmeasured low-x region. The right panel shows the COMPASS result [31] for the helicity DF of valence quarks, $x(u_v + d_v)$, obtained from the semi-inclusive asymmetry of the *difference* of positive and negative pions and kaons, respectively. The first partial moment of this DF in the measured x-range [0.02,0.7] saturates at a value of $0.40 \pm 0.07 \pm 0.05$. From this result it is concluded that the assumption $\Delta\bar{u} = -\Delta\bar{d}$ for the helicity DFs of light sea-quarks agrees much better with the data than the assumption of a flavor symmetric polarized sea: $\Delta\bar{u} = \Delta\bar{d} = \Delta\bar{s} = \Delta s$.

Highlight 9: Gluon helicity distribution The gluon helicity DF $\Delta g(x_g, Q^2)$ can in principle be obtained from NLO-QCD fits to the double-spin asymmetries in inclusive polarized DIS. At present the $x - Q^2$ range of such data is not yet large enough to sufficiently constrain this important quantity. Data at higher values of Q^2 and at lower values of x are urgently needed, which could be obtained by a future polarized electron-proton collider like EIC.

More promising are at present measurements via processes where the gluon density enters the cross section directly. In lepton-nucleon scattering such a process is *photon-gluon fusion* (PGF) ($\gamma^* g \rightarrow q\bar{q}$). This process can be isolated either by studying reactions in which a charmed quark anti-quark pair is produced and the necessary hard scale is given by the mass of the c-quark, or alternatively by measuring a quark and an anti-quark

jet or pairs of hadrons, respectively, or even single hadrons at large transverse momenta p_T relative to the direction of the virtual photon. Results for such measurements have been published by HERMES [32], SMC [33] and COMPASS [34].

DSAs in polarized proton-proton scattering are the second tool to gain direct information about $\Delta g(x_g)$. Several different reaction channels can be studied. Examples are: inclusive jet production, where the dominant partonic subprocesses are $(\vec{g}\,\vec{g} \to g\,g)$ and $(\vec{g}\,\vec{q} \to g\,q)$, inclusive pion production with the same subprocesses, direct photon production corresponding to $(\vec{g}\,\vec{q} \to \gamma\,q)$ and heavy quark production corresponding to $(\vec{g}\,\vec{g} \to c\,\bar{c}, b\,\bar{b})$. These reactions involve a convolution of two parton distributions and the interpretation of the results is therefore always based on a comparison to a Monte Carlo simulation in NLO-QCD. Results for measurement of the longitudinal DSA for inclusive jet and π^0 production have been published by STAR [35] and PHENIX [36] and QCD fits in NLO have been performed to deduce from these results informations about $\Delta g(x)$ [37].

It is difficult to draw a firm conclusion from these results. A large positive gluon distribution is definitively excluded, the data favor a very small Δg, and $\Delta g(x_g)$ possibly has a node at x_g around 0.1. For further detailed discussions see the contributions by E. Leader [18] and E. Rondio [38].

Highlights 10 and 11: Transversity, Collins and Sivers Effect Measurements with transversely polarized targets allow to access transverse-momentum dependent DFs and fragmentation functions (FFs), like the chiral-odd transversity DF $\delta q\,(x, Q^2)$ [39] and Collins FF $H_1^\perp$ [40, 41], which is also odd under naive time reversal, and the time-reversal odd Sivers DF $f_{1T}^\perp$ [42, 43]. One especially interesting aspect of this DF is the possible relation to orbital angular momenta of quarks [44]. Very little experimental information about these quantities exists until now. In SIDIS they manifest themselves in SSAs in the distribution of hadrons in the azimuthal angles ϕ (ϕ_s) around the virtual photon direction between the lepton scattering plane and the hadron production plane (transverse component of the target spin vector). The Collins mechanism will cause a $\sin(\phi + \phi_S)$ moment proportional to a convolution of $\delta q(x)$ and $H_1^\perp(z)$, while the Sivers mechanism will cause a $\sin(\phi - \phi_S)$ moment proportional to the convolution of $f_{1T}^\perp(x)$ and the unpolarized FF $D(z)$.

Preliminary HERMES results [45] for the Collins and Sivers moments for charged pions and kaons, obtained from data taken with a transversely polarized proton target, are shown in Fig. 5. The measured Collins asymmetries (left panel) are small but different from zero providing evidence for the existence of both $\delta q(x)$ and $H_1^\perp(z)$. The large π^- moment indicates that the unfavored Collins FF has similar magnitude as the favored one, but opposite sign.

The π^+ and K^+ Sivers asymmetries (right panel) are significantly positive, providing the first evidence for a T-odd PDF appearing in leptoproduction. Consequently one has to conclude from this result that orbital angular momenta of quarks inside the nucleon are non-zero. At present it is, however, not jet possible to quantitatively relate the magnitude of this asymmetry to the fraction of nucleon spin which can be attributed to orbital angular momenta of quarks. The positive kaon amplitudes appear to be larger than the pion amplitudes, which might point to a large Sivers function for sea-quarks.

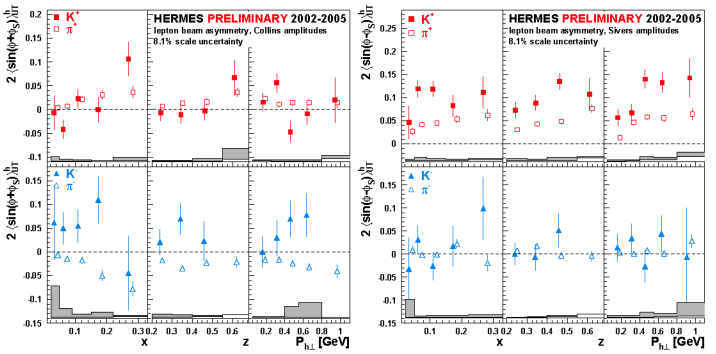

FIGURE 5. HERMES results for the "Collins moments" (left panel) and the "Sivers moments" (right panel) for charged pions and kaons obtained with a transversely polarised hydrogen target.

The COMPASS results [46], obtained from data taken with a polarized deuteron ($\vec{L}i\vec{D}$) target, are compatible with zero within errors for both the Collins and the Sivers moments. Very likely this is caused by cancellations arising a deuteron target. Transversity and Sivers DFs for up-quarks seem to have about the same magnitude as those for down-quarks but opposite sign. Preliminary results from the COMPASS proton data indicate that the Collins moments are different from zero and are in agreement with the HERMES data while the Sivers moments are still compatible with zero. For a detailed discussion of these results and their interpretation see Ref. [47].

Large transverse SSAs or analyzing powers A_N, respectively, have been observed in pp reactions with transverse beam or target spins. For a review of the experimental results and their interpretation see Ref. [48]. Recent theoretical attempts for their interpretation include the role of partonic transverse momentum effects, transversity DF and Collins FF, the Sivers effect, and higher-twist effects arising from quark-gluon correlations [49].

Highlight 12: Hard exclusive processes - Determination of L_q and J_q The partonic structure of the nucleon has traditionally been described in terms of parton distribution functions. In recent theoretical developments these have been conceptually subsumed within the broader framework of Generalized Parton Distributions (GPDs), which also describe elastic form factors and hard exclusive reactions [50]. These distributions allow to obtain a 3-dimensional picture of the nucleon, correlating the longitudinal momentum fraction of partons with their transverse distance from the center of the nucleon. Furthermore moments of certain GPDs were found to relate directly to the total (including orbital) angular momentum carried by partons in the nucleon [51]. GPDs are accessible through hard exclusive processes, i.e. production of vector mesons, pseudoscalar mesons or real photons (Deeply Virtual Compton Scattering, DVCS), that involve at least two hard vertices, yet leave the target nucleon intact. They manifest themselves in various azimuthal angular asymmetries in the azimuthal angles ϕ and ϕ_s with respect to beam charge and beam and target polarization. Several pioneer measurements of various such asymmetries like the beam helicty asymmetry A_{LU}, the beam charge

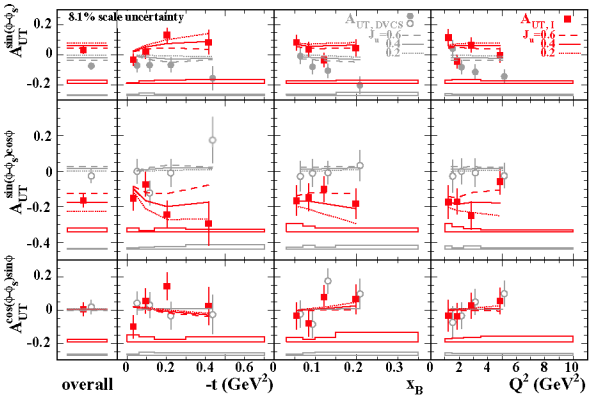

FIGURE 6. HERMES results for the asymmetry amplitudes in DVCS for the transversely polarized proton target.

asymmetry A_C, and the longitudinal (transverse) target spin asymmetry $A_{UL}(A_{UT})$ for DVCS or the transverse target asymmetry A_{UT} for ρ^0 and π^+ mesons have been performed by HERMES [52, 53] [53] and JLAB [54]. As an example various moments of the transverse target asymmetry A_{UT} are shown in Fig. 6 as a function of the kinematic variables $-t, x_B, Q^2$. The data show some (model-dependent) sensitivity to the total up-quark angular momentum J_u. The ultimate goal of such investigations is to constrain and to evaluate the up- and down-quark total (orbital) angular momentum contribution to the spin of the nucleon. HERMES has performed further measurements with a dedicated recoil detector and several 2nd generation experiments are presently being planned and prepared for future high precision measurements of this kind.

CONCLUSION

Spin experiments have produced exciting results which are often a challenge for theory. I am looking forward to see plenty even more challenging results from the next generations of high precision spin experiments.

REFERENCES

1. A. Blondel et al., Proceedings of the 12th Intrnational Symposium on High-Energy Spin Physics, 10-14 September 1996, Amsterdam, C.W. de Jager et al. (Eds.), 267-271 ((1997).
2. D. Barber et al., *Nucl. Instrum. Meth.* **A338**, 166-184 (1994).
3. D. Barber et al., *Phys. Lett.* **B343**, 436-443 (1995).
4. A. Zelensky, these Proceedings
5. W. Haeberli and E. Steffens, *Rep. Progr. Phys.* **66**, 1887-1935 (2003).
6. W. Meyer, these Proceedings
7. T. Roser, these Proceedings
8. J. Clarke, these Proceedings

9. E. Steffens, these Proceedings
10. R. Prepost, Proceedings of the 12th Intrnational Symposium on High-Energy Spin Physics, 10-14 September 1996, Amsterdam, C.W. de Jager et al. (Eds.), 127-135 ((1997).
11. C. Amsler et al., *Phys. Lett.* **B667**, 1(2008).
12. P. L. Anthony et al., *Phys. Rev. Lett.* **95**, 081601 (2005).
13. D. S. Armstrong et al., *Phys. Rev. Lett.* **95**, 0892001 (2005).
14. J. Liu et al., *Phys. Rev.* **C76**, 025202 (2007).
15. A. Acha et al., *Phys. Rev. Lett.* **98**, 032301 (2007).
16. A. Aktas et al., *Phys. Lett.* **B632**, 35 (2006).
17. S. Chekanov et al., *Eur. Phys. J.* **C42**, 1 (2005); DESY-08-177 (2008).
18. E. Leader, these Proceedings.
19. C. Hyde and K. de Jager, *Ann. Rev. Nucl. Part. Sci.* **54**, 217 (2004).
20. P. Guichon and M. Vanderhaeghen, *Phys. Rev. Lett.* **91**, 142303 (2003).
21. E. B. Hughes et al., *Phys. Rev.* **B139**, 458 (1965).
22. E. Geis et al., *Phys. Rev. Lett.* **101**, 042501 (2008).
23. F. Rathmann et al., *Phys. Rev.* **C58**, 658 (1998).
24. M. Burkardt, A. Miller, and W.-D. Nowak, arXiv:0812.1234 (2008).
25. W. Vogelsang, private communication.
26. A. Airapetian et al. (HERMES), *Phys. Rev.* **D75**, 012007 (2007).
27. V.Yu. Alexakhin et al. (COMPASS), *Phys. Lett.* **B647**, 8-17 (2007).
28. J. Ashman et al. (EMC), *Phys. Lett.* **B206**, 364 (1988).
29. A. Airapetian et al. (HERMES), *Phys. Rev.* **D71**, 012003 (2005).
30. A. Airapetian et al. (HERMES), *Phys. Lett.* **B666**, 466 (2008).
31. M. Alekseev et al. (COMPASS), *Phys. Lett.* **B660**, 458-465 (2008).
32. A. Airapetian et al. (HERMES), *Phys. Rev. Lett.* **84**, 2584-2588 (2000).
33. B. Adeva et al. (SMC), *Phys. Rev. D* **70**, 012002 (2004).
34. E.S. Ageev et al. (COMPASS), *Phys. Rev. D* **70**, 012002 (2004); *Phys. Lett. B* **633**, 25-32 (2006); M. Alekseev et al. (COMPASS), arXiv:0802.3023 (2008).
35. B.I. Abelev et al. (STAR), *Phys. Rev. Lett.* **97**, 252001 (2006); *Phys. Rev. Lett.* **100**, 232003 (2008).
36. S.S. Adler et al. (PHENIX), *Phys. Rev.* **D73**, 091102 (2006); A. Adare et al. (PHENIX), *Phys. Rev.* **D76**, 051106 (2007); arXiv:0810.0694(2008).
37. D. de Florian et al., *Phys. Rev. Lett.* **101**, 072001 (2008).
38. E. Rondio, these Proceedings.
39. V. Barone and P.G. Ratcliffe, *Transverse Spin Physics*, World Scientific, 2003.
40. J. Collins, *Nucl. Phys. B* **396**, 161-182 (1993).
41. J. Collins et al., *Nucl. Phys. B* **420**, 565-582 (1994).
42. P. J. Mulders and R. D. Tangerman, *Nucl.Phys. B* **461**, 197-237 (1996); Erratum *Nucl.Phys. B* **484**, 538-540 (1997).
43. D. W. Sivers, *Phys. Rev. D* **41**, 83-90 (1990); *Phys. Rev. D* **43**, 261-263 (1991).
44. M. Burkardt, *Phys. Rev. D* **66**, 114005 (2002), *Phys. Rev. D* **69**, 074032 (2004).
45. M. Diefenthaler (for the HERMES collaboration), Proceedings of the 15th International Workshop on Deep-Inelastic Scattering (DIS2007), 16-20 April 2007, 579-582 (2007).
46. V.Yu. Alexakhin et al. (COMPASS), *Phys. Rev. Lett.* **94**, 202002 (2005).
47. N. Makins, these Proceedings
48. C. Aidala, arXiv:0808.4139 (2008) and these Proceedings
49. J. Qiu and G. Sterman, *Phys. Rev.* **D59**, 014004 (1999); M. Anselmino et al., *Phys. Lett.* **B362**, 164 (1995); M. Anselmino et al., *Phys. Rev.* **D60**, 054027 (1999); Y. Koike, *AIP Conf. Proc.* **675**, 449 (2003).
50. C. Weiss, these Proceedings
51. X.D. Ji, *Phys. Rev. Lett.* **78**, 610 (1997).
52. A. Airapetian et al. (HERMES), *Phys. Rev. Lett.* **87**, 182001 (2001); *Phys. Rev.* **D75**, 011103 (2007).
53. A. Airapetian et al. (HERMES), *JHEP* **0806**, 66 (2008).
54. S. Stepanyan et al. (CLAS), *Phys. Rev. Lett.* **87**, 1820012 (2001); S. Chen et al. (CLAS), *Phys. Rev. Lett.* **97**, 072002 (2006); C. Munoz Camacho et al. (JLAB Hall A), *Phys. Rev. Lett.* **97**, 262002 (2006); F.X. Girod et al.(CLAS), *Phys. Rev. Lett.* **100**, 162002 (2008).